# Power-Efficient Hybrid Energy Harvesting System for Harnessing Ambient Vibrations

Salar Chamanian, *Member, IEEE*, Berkay Çiftci, *Student Member, IEEE*, Hasan Uluşan, *Member, IEEE*, Ali Muhtaroğlu, *Senior Member, IEEE*, and Haluk Külah, *Member, IEEE*

***Abstract*— This paper presents an efficient hybrid energy harvesting interface to synergistically scavenge power from electromagnetic (EM) and piezoelectric (PE) sources, and drive a single load. The EM harvester output is rectified through a self-powered active doubler structure, and stored on a storage capacitor. The stored energy is then transferred to the PE harvester to increase the damping force and charge extraction. The total synergistically extracted power from both harvesters is more than the power obtained from each independently. The hybrid operation is validated through a compact and wearable platform that includes custom designed EM and PE harvesters for scavenging energy from human motion. The system supplies 1–3.4 V output for powering up wireless sensor nodes with a wide range of vibration frequency, and generates between 1–100 $\mu$W at 90% maximum power conversion efficiency. The solution has superior power generation performance compared to previous stand-alone systems in the literature.**

***Index Terms*— Self-powered, vibration, hybrid harvester, piezoelectric energy harvester, electromagnetic energy harvester, IC.**

## I. Introduction

RECENT developments in electronic circuits have made low-power wireless sensor networks (WSNs) widely available for smart buildings, automotive industry, and implantable electronics [1], [2]. Although low-power design techniques prolong the operation of WSNs, size-limited batteries utilized to supply power to the sensor nodes constrain their lifetimes. Battery volume does not diminish at the same rate as the sensor electronics, and thus forms the bulk of the system [2]. Besides, replacement and maintenance of these batteries can be costly and practically unattainable due to the location of the sensor or increasingly large number of sensor nodes [3]. A feasible solution to extend the lifetime of a WSN node is scavenging energy from ambient energy sources to recharge the battery, or to operate without batteries [4].

Different methods, namely photovoltaic, vibrational, thermal, and RF have been proposed to harvest available energy in the environment [2], [5]. Several transducers and power management circuits have been designed and fabricated to harvest energy from a single source, and convert it into usable forms [6]–[9]. However, depending on a single energy source to power up WSNs reduces the system reliability [10] due to the fact that most energy sources are unpredictably intermittent. Therefore, an efficient hybrid configuration, in which the system extracts power from different energy sources synergistically, can improve endurance and reliability of the WSN operation.

Over the last decade, various hybrid energy harvester and interface designs have been proposed to extract energy from environmental sources. There exist two common approaches in the literature: voltage adding and shared inductor. Output voltage adding technique depicted in Fig. 1(a) comprises an individual interface circuit for each energy harvester and addition of generated output voltage signals to drive a single load [12], [23]. Although it has a simple control, this topology imposes limitations due to interaction between individual ICs at the output stage, and reduces the overall efficiency of the hybrid system. The energy generated by each harvester in the multi-input system is initially stored on its own buffer capacitor in the shared inductor technique illustrated in Fig. 1(b). The relatively complex sequential control requires fine adjustment to effectively employ an off-chip inductor to time-multiplex the transfer of energy from each harvester to the load without wasting extractable energy [10], [24]. In [10], a harvesting platform contains dual-path architecture to combine three different energy sources (solar, thermal, and vibration). A shared inductor topology is used to extract energy from each source in sequence. This circuit wastes energy and impose limitations for low-input excitation conditions. The system proposed in [11] combines RF and thermoelectric power sources to sustain a micro-battery. Despite the fact that the system is able to extract power from two separate energy sources, simultaneous or synergistic power extraction is not achievable. The hybrid system represented in [12] utilizes solar and vibration energy sources for the purpose of delivering power to distinct loads determined by a switch matrix. This

Manuscript received September 20, 2018; revised January 10, 2019 and February 16, 2019; accepted February 16, 2019. Date of publication March 15, 2019; date of current version June 18, 2019. This work has received funding from the European Research Council (ERC), under the European Union's Horizon 2020 Research and Innovation Programme (Grant 682756) and was supported in part by the Scientific & Technical Research Council of Turkey (TUBITAK) under Grant 117E003. This paper was recommended by Associate Editor A. Fayed. *(Corresponding author: Salar Chamanian.)*

S. Chamanian, B. Çiftci, and H. Uluşan are with the Department of Electrical and Electronics Engineering, Middle East Technical University, 06800 Ankara, Turkey (e-mail: salar.chamanian@metu.edu.tr; cberkay@metu.edu.tr; hulusan@metu.edu.tr).

A. Muhtaroğlu is with the Center for Sustainability, Middle East Technical University Northern Cyprus Campus, 99738 Güzelyurt, Turkey (e-mail: amuhtar@metu.edu.tr).

H. Külah is with the Department of Electrical and Electronics Engineering, Middle East Technical University, 06800 Ankara, Turkey, and also with the METU-MEMS Research and Application Center, 06800 Ankara, Turkey (e-mail: kulah@metu.edu.tr).

Color versions of one or more of the figures in this paper are available online at http://ieeexplore.ieee.org.

Digital Object Identifier 10.1109/TCSI.2019.2900574

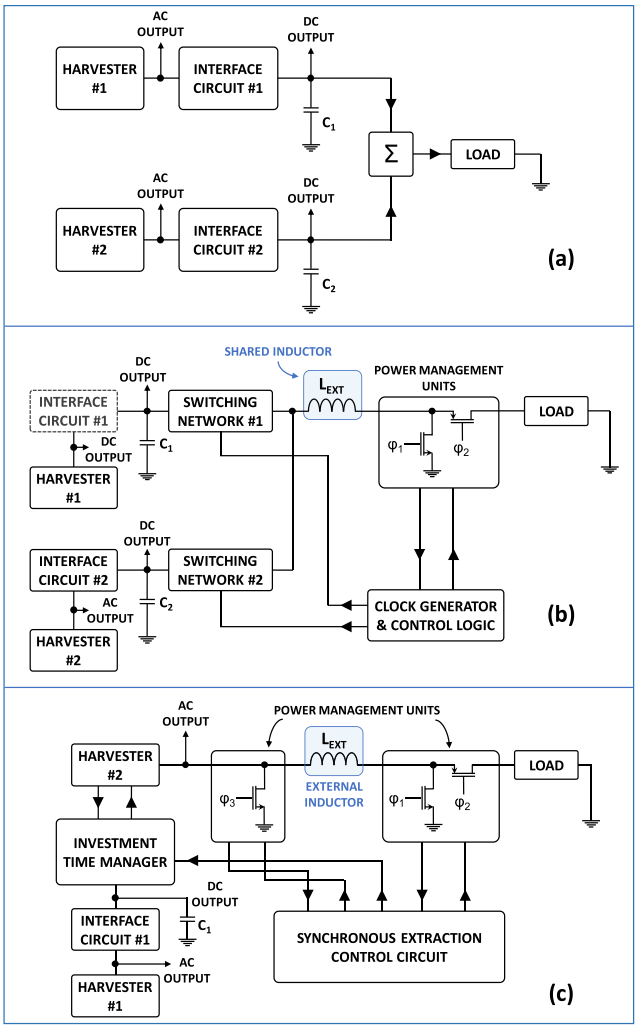


Fig. 1. System architectures of conventional hybrid harvester interfaces using (a) output voltage adding, (b) shared inductor techniques, and (c) proposed system configuration which offers synergistic extraction.

design is able to add output voltages of two harvesters as an input to a DC-DC converter, but it is not focused on power conversion and hybridization of the harvesters.

Scavenging of environmental vibrations is a promising approach to power up WSNs through piezoelectric and electromagnetic energy harvesters. In the literature, there are different electronic systems for harnessing low frequency vibrations through electromagnetic harvesters [8], [13], and high frequency vibrations through piezoelectric harvesters [14]–[20]. Full-wave diode-bridge rectifier is the most common converter, which has been implemented to convert piezoelectric AC voltage to usable DC voltage. To enhance power efficiency, maximum power point tracking methods [16], [17], [19], [20] are utilized to match load impedance of the full bridge rectifier to the real part of the source impedance.

Nevertheless, harvesting energy from both low and high frequencies in a hybrid scheme are more beneficial in terms of increased power capacity, which in turn improves lifetime and system reliability compared to single source input system. A vibration-based harvesting system presented in [21] combines electromagnetic and piezoelectric energy to achieve a hybrid structure. The main concern in this system is that it can harvest only from a single vibration source; otherwise, the system operation fails. The triple hybrid power generator proposed in [22] has inputs from three different sources, and can extract power from each one at the same time to supply a DC voltage. Nevertheless, the system can only provide output voltage level around 1 V in an extremely narrow range. Moreover, power conversion efficiency of the system is relatively low in this design.

In this paper, a hybrid system is proposed to combine piezoelectric energy harvesters with electromagnetic energy harvesters or any harvester with DC output to enhance energy extraction from vibrations. Fig. 1(c) shows architecture of the proposed circuit. In contrast to conventional hybrid systems, the energy integration and extraction are realized in synchrony with the incoming energy at the energy harvester interface. Synchronous operation of energy integration has been achieved through investment time manager. This unit contains charge investment path, and controls timing as well as investment. Investment time manager acts in interaction with the synchronous energy extraction circuit. The proposed circuit with novel energy integration method enables energy extraction from two energy sources at the same time with high efficiency. The system has a broad operation range between few $\mu$Ws available from body motion to more than 100 $\mu$W generated from high frequency excitations. The hybrid system is suitable for wearable applications, and can be carried on a human wrist to collect energy from body movements. A novel power management circuit is designed to extract energy from two energy sources at the same time with high efficiency. This paper is organized as follows: Section II describes system operation in detail. Section III discusses experimental results from the fabricated IC for high piezoelectric excitation frequencies. Section IV presents the wearable energy harvesting system with measurements in an application like environment. Finally, Section V concludes the paper.

## II. Hybrid System Architecture

### A. Operation Principle of the Proposed System

Scavenging energy from both electromagnetic (EM) and piezoelectric (PE) energy harvesters in a hybrid structure can enhance the extracted output power, as available vibration sources exist at low and high frequencies in the environment. Both EM and PE harvesters produce AC outputs, and need rectification and power management circuits to accumulate extracted charge on a single storage element. The output impedance of PE harvesters is capacitive and relatively high. The generated charge is stored within piezoelectric capacitance $C_{PZT}$ which provides a relatively high output voltage with a relatively low current level. The high output impedance impedes efficient power transfer with the conventional AC/DC conversion techniques, and summons the need for an impedance matching interface. On the other hand, EM harvesters produce high output current as the magnetic fluctuation directly induces an electrical current on the coil winding. Low output voltage resulting from low output impedance presents different challenges for EM energy harvesting interface design compared to PE harvesting.

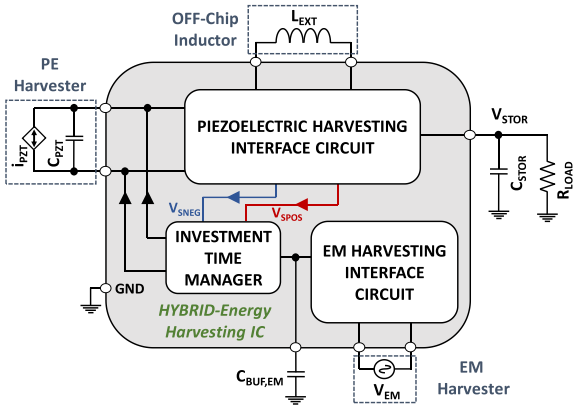


Fig. 2. System architecture of the vibration-based hybrid harvester interface.

The main goal is to increase power capacity of energy harvesting system through combination of PE and EM harvesters without degrading harvesters' performance. The key idea in proposed architecture is integration of energy on piezoelectric harvester in synchrony with the incoming energy to secure synergistic and load independent energy extraction. This is achieved through investment time manager circuit in cooperation with synchronous energy extraction circuit, and EM harvesting interface circuit.

The proposed hybrid interface circuit, composed of three building blocks, is presented in Fig. 2. The system utilizes power from EM harvester to invest energy to PE harvester in order to increase the damping force. The harvested energy from EM harvester is then transferred to the storage element concurrently with the energy extracted from the PE harvester. EM harvester interface circuit (EM-IC) rectifies AC voltage through a self-powered voltage doubler with active diodes. PE harvester interface circuit (PEH-IC) is designed based on Synchronous Electric Charge Extraction (SECE) technique due to the fact that this topology provides a load independent structure for fast-charging the storage element with a wide range of output voltage. The circuit manages timing to share the charge on EM buffer capacitance, $C_{BUF,EM}$ with PE capacitor, $C_{PZT}$. This leads to an improvement in the electromechanical coupling factor of piezoelectric harvester, and hence in the total power extraction compared to sum of output power from two harvesters. The piezoelectric electromechanical coupling factor is a measure for the part of mechanical energy that is converted into electrical energy. It simply relates mechanical stress to electrical field in piezoelectric energy harvester. In implemented SECE technique, the piezoelectric harvester is put into open circuit condition by turning all switches OFF to isolate the piezoelectric harvester from the storage capacitor. In this state, there is no conduction between the piezoelectric and output, and all generated charge is stored on $C_{PZT}$. Once piezoelectric harvester reaches its peak displacement at T/2, all accumulated charge at $C_{PZT}(V_{PP}C_{PZT})$ is transferred to the inductor and then delivered to the storage capacitor through the switching sequence. Therefore, the achieved average extracted energy can be represented as:

$$E_{PZT1} = \frac{1}{2} C_{PZT} V_{PP}^2, \tag{1}$$

where $V_{PP}$ is the voltage difference between two terminals of the PE harvester generated at each half cycle. The PE IC tracks maximum power point automatically and can provide more power for low-coupled harvesters in comparison with the maximum power that a lossless full-wave diode-bridge rectifier at each half-cycle can output [16], $E_{FB,max} = C_{PZT} V_p^2$, where $V_P$ is the peak amplitude of the PE voltage. The dependency of the power gain achievable by SECE compared to the full-wave rectifier has its origin in the coupling force amplitude. $V_{PP}$ is close to twice the $V_P$ for low-coupled piezoelectric harvesters or off-resonance excitations. Therefore, the SECE interface is capable of increasing the harvested power to about 400% of a lossless full-wave rectifier.

In the proposed system, the circuit invests charge into $C_{PZT}$ from $C_{BUF,EM}$ at minimum or maximum displacement of the harvester after charge extraction. Assume $\boldsymbol{\Delta V}$ is added up on $C_{PZT}$ before PE beam starts its positive or negative swing. After the full swing of the PE harvester, $V_H = V_{PP,H} + \Delta V$ accumulates on $C_{PZT}$, resulting in extractable energy from harvester as:

$$\begin{aligned} E_H &= \frac{1}{2} C_{PZT} V_H^2 = \frac{1}{2} C_{PZT} (V_{PP,H} + \Delta V)^2 \\ &= \frac{1}{2} C_{PZT} V_{PP,H}^2 + \frac{1}{2} C_{PZT} \Delta V^2 + C_{PZT} V_{PP,H} \Delta V \end{aligned} \tag{2}$$

where $1/2 C_{PZT} V_{PP,H}^2 \cong E_{PZT1}$ is the energy generated on $C_{PZT}$ without any investment, $1/2 C_{PZT} \Delta V^2 = E_{INV}$ is the invested energy from EM harvester output, and $C_{PZT} V_{PP,H} \Delta V = E_{GAIN}$ is the augmenting energy extracted due to the squared relation of generated energy to the voltage. It can be analytically observed from equation (2) that apart from the individual outputs of each harvester, augmenting energy, $E_{GAIN}$ can be generated on $C_{PZT}$, which improves the output power of the hybrid system. EM output voltage level is low at moderate vibrations. Therefore, the main focus of the EM harvester interface design is the efficient rectification and boosting of the EM output voltage. Maximum power point tracking is not as relevant for the EM transducer with low output impedance. Since invested charge is transferred synergistically with piezoelectric charge, the proposed hybrid system delivers power independent of the output load. As a result, proposed hybrid architecture can synergistically extract more power from two different harvesters compared to voltage adding [12], [23] and inductor sharing techniques [10], [24].

### *B. EM Harvesting IC*

Environmental vibrations can occur both at low and high frequency domains. Inertial mass of EM harvesters enables capturing of low frequency and low profile ambient vibrations with limited output voltage amplitude, which requires efficient rectifier circuits to minimize losses. The AC voltage harvested from low frequency vibrations is efficiently converted into DC through an interface circuit that both rectifies and boosts the input voltage. The utilized EM harvester interface circuit depicted in Fig. 3 is a modified version of the one presented in [13]. The rectification of the input signal is handled through an active diode that provide forward voltage-drop close to that of an ideal rectifier. The comparator in the active diode

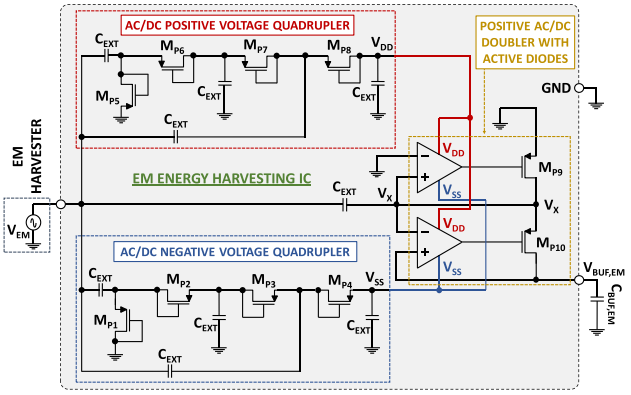


Fig. 3. Self-powered EM energy harvesting interface circuit for low frequency vibrations.

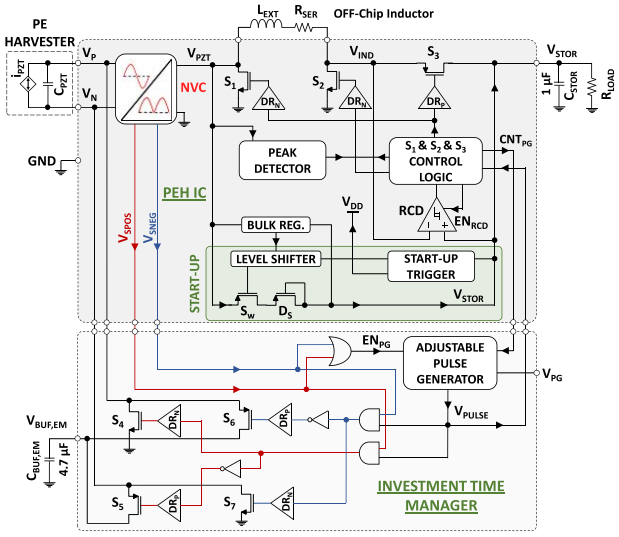


Fig. 4. Schematic of PE energy harvesting interface circuit (PEH-IC) and investment time manager.

is powered by passive AC/DC quadrupler structures which are also driven by the EM harvester. Although the passive diode structure leads to higher voltage drop compared to active diodes, the quadrupler provides sufficient voltage and current (only several tens of nano-Amps) to drive the comparators. The result is fully self-powered operation with low drop-out voltage and low $I^2R$ losses. The positive quadrupler delivers high enough voltage to turn off the pMOS switch with low leakage current, while the negative quadrupler reduces path resistance to drive current through high source-to-gate voltage. For negative input voltages with $V_x$ < GND, switch $M_{P9}$ is turned ON by the corresponding comparator and charges the external capacitor until the negative input peak. When $V_x$ > GND, the $M_{P9}$ switch is turned OFF and the charge is stored on the capacitor. For positive input voltages with $V_x > V_{BUF,EM}$, the $M_{P10}$ switch is turned ON, and the output capacitor ($C_{BUF,EM}$) is charged until two times the input peak voltage. When $V_x$ goes below $V_{BUF,EM}$, the switch $M_{P10}$ is turned OFF to preserve the maximum charge at the output. The utilized comparators are designed to obtain single-ended output with high gain and sensitivity, and minimize forward voltage drop between source and drain of the active switches. The off-chip external capacitors for passive and active parts have been chosen as 1 and 4.7 $\mu$F, respectively, to provide efficient charging and high storage power at the output capacitor $C_{BUF;EM}$. Threshold voltage of the MOSFETs that make up the passive circuit is a critical parameter to determine the voltage conversion efficiency. Thus, low voltage threshold (LVT) MOSFETs with about 0.35 V threshold voltage are utilized in this part. On the other hand, the switches in the active diodes ($M_{P9}$ and $M_{P10}$) have higher voltage compliance and 3.3 V MOSFETs with ~0.6 V threshold voltage are utilized. Power loss in the passive rectifier (<0.5 $\mu$W) is much lower than the generated EM output power; hence the power conversion efficiency is not affected by the power dissipation of this stage. Although, most of the power dissipation of the circuit is in the active part, the high drive capacity of the active diodes enables more than 70% power conversion efficiency for the overall EM harvesting IC.

### *C. PE Harvesting IC and Investment Time Manager*

PE harvesting interface circuit operates in synchrony with investment time manager to facilitate charge transfer from EM buffer capacitance. PE harvesting interface circuit consists of a negative voltage converter (NVC), start-up block, three detectors, and switch control logic similar to our previous work [25], as shown in Fig. 4. Investment time manager regulates the energy integration in the proposed architecture. It comprises an adjustable pulse generator, investment switches ($S_4$, $S_5$, $S_6$, and $S_7$), and control logic. It provides synchrony through interaction with NVC and piezoelectric extraction circuit. The invested charge from the EM harvester to the PE harvester is adjustable to regulate the EM harvesting output, and also controls the damping force of the PE harvester.

*1) Negative Voltage Converter:* NVC generates a peak-to-peak open circuit voltage in each half cycle. Two switches controlled by two comparators and two cross-coupled pMOS switches driven by piezoelectric harvester determine the charge-flow path to provide positive voltage. A current-follower input stage that monitors piezoelectric voltage following by a common-source stage form the comparator as shown in Fig. 5. The transistor sizes are determined to provide required gain within subthreshold biasing region, and an offset is imposed by slightly mismatching the aspect ratio of $M_3$ and $M_4$ MOSFETs to avoid premature switching during transition. Mismatch is adjusted at differential stage through simulations to achieve 20 mV offset. The rising edge of each comparator output indicates maximum and minimum displacement that shorts lower-potential terminal of the harvester to ground.

The storage capacitance is initially charged via the NVC, a diode, and a switch controlled by the start-up circuit. The circuit continuously monitors the storage voltage $V_{STOR}$ and powers up the control unit when it exceeds the minimum required value of 1.1 V.

*2) PZT Harvesting Phases:* At wake-up, the positive voltage from NVC (via cross-coupled pMOS switches) charges the storage capacitor, $C_{stor}$, through a diode $D_S$ and a control pMOS switch $S_W$. The startup trigger circuit decouples the supply voltage of the control unit ($V_{DD}$) and storage voltage ($V_{stor}$) as long as $V_{stor} < V_{trig}$, and switches the storage voltage to power up the active components in the control unit

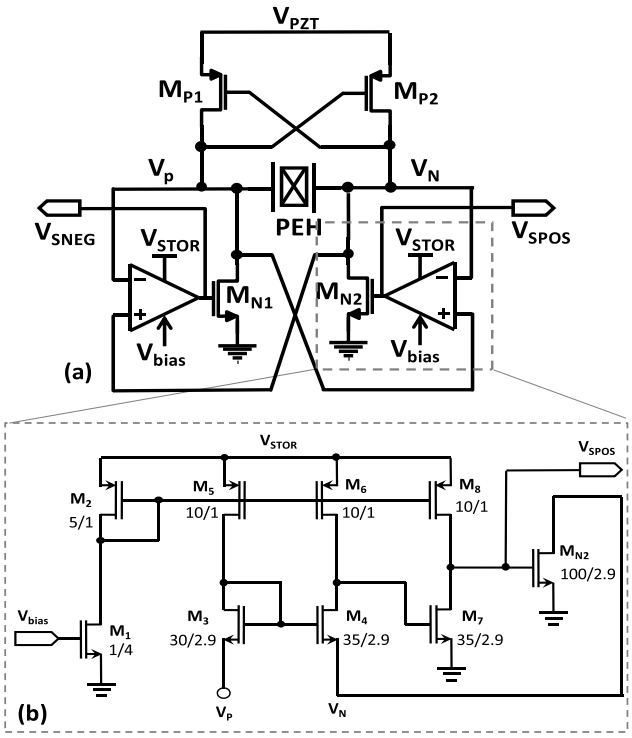


Fig. 5. Schematic of (a) the proposed negative voltage converter (NVC), (b) the comparator utilized inside NVC structure.

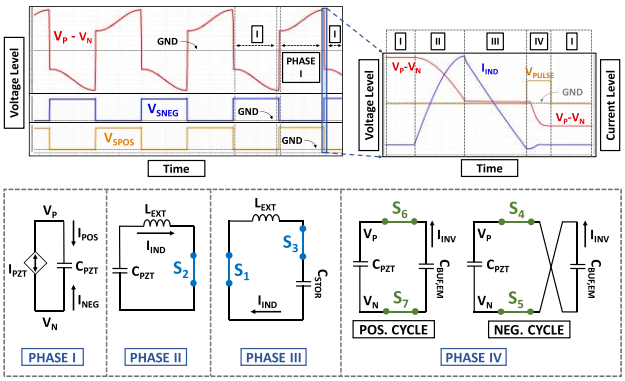


Fig. 6. Summary of operation phases for PE energy harvesting interface circuit and investment time manager.

($V_{DD}$ =$V_{stor}$) when $V_{stor} > V_{trig}$. Energy extraction is realized through four phases of switching as shown in Fig. 6. In phase I, all the switches are OFF, and voltage across PE capacitor is increasing due to charge generation on piezoelectric material. As peak instant is sensed by the peak detector (PD), the circuit initiates phase II by turning the switch $S_2$ ON. The operation of the PD was extensively analyzed in [25]. At this point, charge generated on $C_{PZT}$ is transferred to the external inductor due to the establishment of LC resonance circuit. Zero-crossing detector (ZCD) outputs a signal when rectified piezoelectric voltage $V_{PZT}$ drops below zero to terminate charge extraction. In phase III, extracted charge is transferred from inductor to the storage capacitance $C_{STOR}$ by turning $S_2$ OFF and $S_1$ & $S_3$ ON. Charging of $C_{STOR}$ is completed as stored charge starts flowing back from $C_{STOR}$ to the inductor. A reverse current detector (RCD) monitors voltage drop on

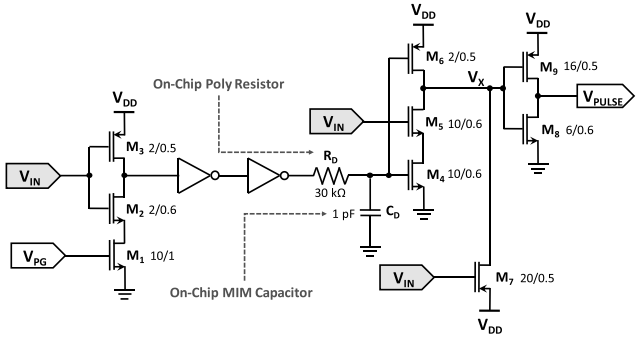


Fig. 7. Schematic of the adjustable pulse generator.

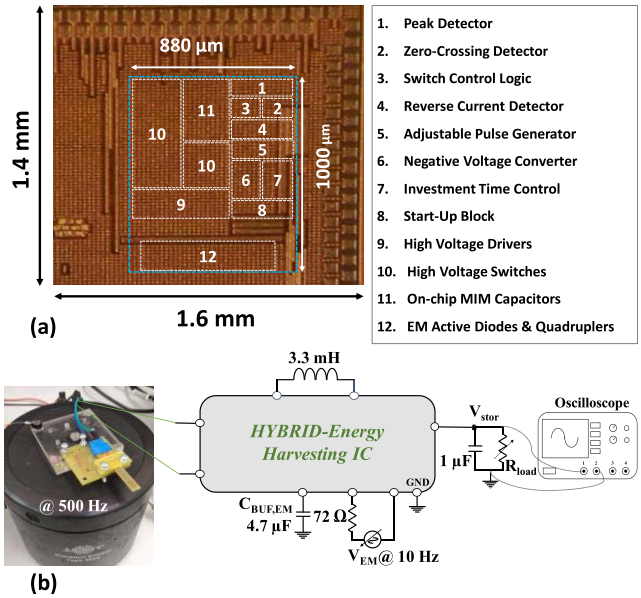


Fig. 8. (a) Die micrograph of the implemented hybrid interface circuit fabricated in 0.18 $\mu$m HV CMOS technology and (b) experimental setup.

$S_3$ to signal end of phase III. The RCD is only activated in phase III to save power. Charge investment is performed during phase IV. The rising edge of $V_{SPOS}$/$V_{SNEG}$ of NVC initiates charge investment by triggering an adjustable pulse generator. The circuit utilizes control signals $V_{SPOS}$/$V_{SNEG}$ to identify piezoelectric polarity, and manages $S_4$–$S_5$ and $S_6$–$S_7$ switch pairs to invest charge from $C_{BUF,EM}$ onto $C_{PZT}$ in reverse and direct polarity corresponding to the piezoelectric displacement. The circuit thus secures augmentation effect between $V_{PP}$ and $\Delta V$ at all times. Investment time manager applies a pulse to invest charge into piezoelectric capacitance with controlling switch network corresponding to downward or upward displacement. The system can operate even when EM harvester delivers very low power and voltage. Since switches within the investment time manager are powered using the energy stored at the output, available instantaneous EM power does not impact the performance of the time manager circuit.

*3) Investment Time Manager:* Investment time manager generates a pulse to invest charge into piezoelectric capacitance with a controlling switch network corresponding to downward or upward displacement. $CNT_{PG}$ signal indicates

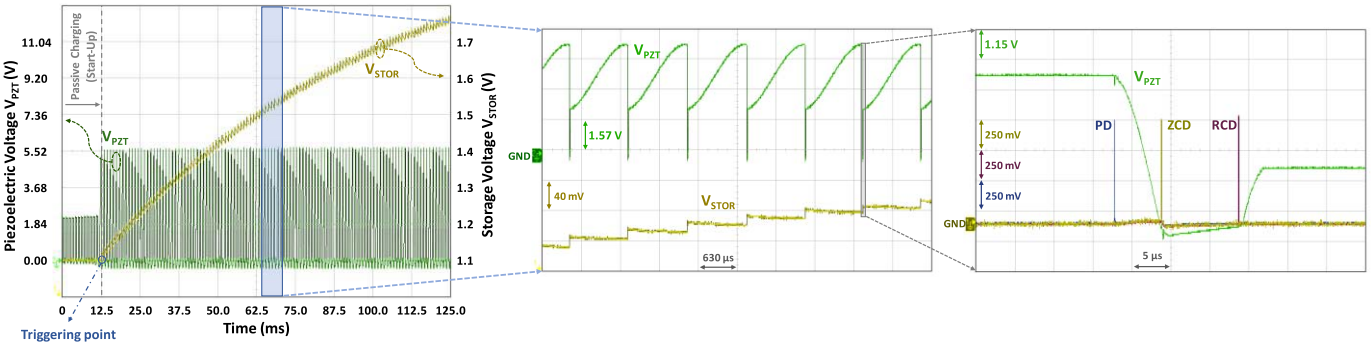


Fig. 9. Measured waveforms of the hybrid harvesting interface operation with generated control signals PD, ZCD, and RCD.

charge depletion at the PE harvester which is a necessary condition for charge investment. The rising edge of $V_{SPOS}/V_{SNEG}$ of NVC initiates charge investment in phase IV by triggering an adjustable pulse generator. The circuit utilizes control signals $V_{SPOS}/V_{SNEG}$ to identify piezoelectric polarity, and manages $S_4$–$S_5$ and $S_6$–$S_7$ switch pairs to invest charge from $C_{BUF,EM}$ onto $C_{PZT}$ in reverse and direct polarity corresponding to the piezoelectric displacement. The circuit thus secures augmentation effect between $V_{PP}$ and $\Delta V$ at all times. The falling edge of the pulse ends the investment and the circuit goes back to phase I to initiate a new cycle.

Adjustable pulse generator circuit is implemented as shown in Fig. 7 to control the time interval of charge investment. The circuit uses inverters and R-C components to set delay time. A current-controlled inverter adjusted with external bias is also utilized for delay-tuning and post-fabrication compensation of any variation from process and temperature. Besides, the pulse width is adjusted to highest possible voltage at $C_{BUF,EM}$ to secure sufficient time for charge investment and proper operation. As the input transitions high, $M_7$ and $M_5$ trip and $M_4$ is still ON so that $V_x$ is discharged through $M_4$ and $M_5$ to generate rising-edge of a pulse. $M_4$ and $M_6$ start to trip within the delay time and $M_7$ pulls $V_x$ up. As result, output falls to generate the output pulse width. All components, including the resistor and the capacitor, are embedded into the chip.

## III. Design Validation

Fig. 8(a) presents the die micrograph of EM and PE harvesting interface circuits fabricated in 0.18 $\mu$m HV CMOS technology. The first experiment verifies operation of the proposed system with the assumption that two independent vibration sources are available at lower and higher frequency bands. A PE harvester (MIDE V22BL with series connection) with a 4.7 nF capacitor is excited with shaker table and EM is emulated by an AC voltage source with a 72 Ω series resistor. An inductor $L_{EXT} = 3.3$ mH/8.97 Ω with 125 mm$^3$ package, and a storage capacitor with $C_{stor} = 1$ $\mu$F are externally connected to the circuit as shown in Fig. 8(b). A high inductance value in the same package is preferred to reduce the magnitude of the oscillation current, $I_{IND,m} = V_{PP}\sqrt{C_{PZT}/L_{EXT}}$ passing through the switches and the inductor as shown in Fig. 6. This decreases the total conduction power loss during phase I and phase II, and consequently improves overall power conversion efficiency.

Fig. 9 shows measured waveforms of the hybrid interface operation while PE and EM harvesters are excited at 500 Hz and 10 Hz, respectively. The piezoelectric open circuit voltage is set to 3.45 $V_{PP}$. The hybrid IC invests harvested energy from $C_{BUF,EM} = 4.7$ $\mu$F buffer capacitance to $C_{PZT} = 4.7$ nF, and transfers available charge on PE harvester to 1 $\mu$F storage capacitor. Fig. 10 depicts the charging profile of a 1 $\mu$F capacitor in parallel with 150 kΩ load resistor for different outputs of EM harvesting system. Initially, the storage voltage is observed to be stabilized for PE harvester excitation at 500 Hz with PE open circuit voltage $V_{OC} = 4.4$ $V_{PP}$ and without any charge investment from EM harvesting circuit. Then, hybrid operation is enabled to monitor the charging performance of the proposed IC for different input power levels supplies from the EM harvester. The hybrid IC transfers the stored charge from EM buffer capacitor to the storage capacitor, thus reinforcing power output.

Measured extracted power as a function of peak-to-peak PE open circuit voltage for different power values at EM interface input is depicted in Fig. 11. The hybrid system outputs more power (red, green, and gray) in comparison with the accumulation of standalone extracted output power figures as can be observed in Fig. 11. Indeed, investing charge raises the electrostatic damping force in the piezoelectric harvester. This additional force works against vibrations to reduce the beam displacement as shown in Fig. 12 for different investment power levels. The system draws more power from motion as a result of the increased damping force, which consequently increases power transferred to the output, and leads to higher power conversion efficiency.

Fig. 13 shows measured power conversion efficiency ($\eta = P_{OUT}/P_{IN}$) for hybrid IC and stand-alone interface circuits. As expected, power conversion efficiency increases with the charge investment from EM harvester based on the elevated damping of the PE harvester. Switching, driving and conduction are the main sources of power loss. Besides, the quiescent current is measured by fixing $V_{Stor}$ through an external supply and measuring the drawn current while the IC is not performing any energy extraction. The IC draws an average of 280 nA across its operating voltage range from 1 to 3.3 V. The dynamic average power consumption of the control components, which are activated during the energy extraction, ranges between 100 nA and 160 nA, depending on the input power level. Lower efficiency is observed at low

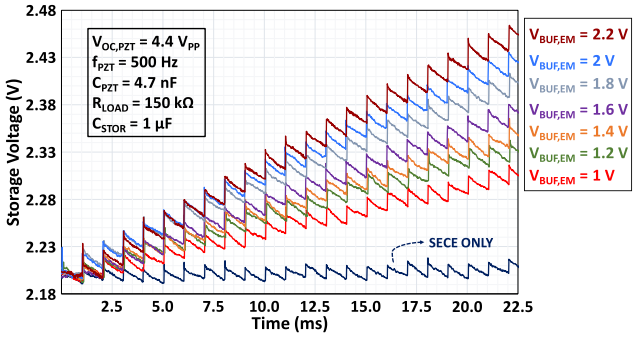


Fig. 10. Measured charge profile of a 1 $\mu$F load capacitor for different outputs of EM harvesting interface circuit.

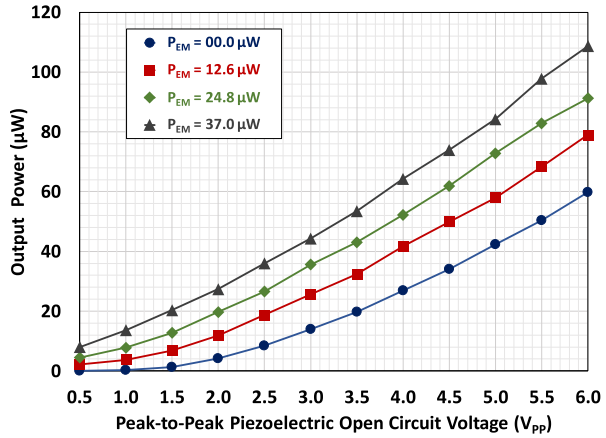


Fig. 11. Extracted power vs. peak-to-peak piezoelectric open circuit voltage for high frequency excitations.

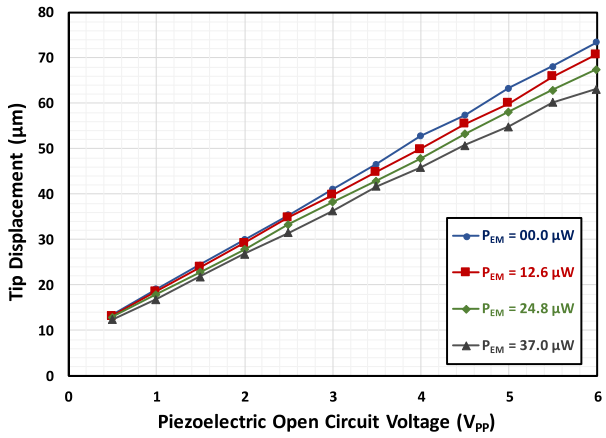


Fig. 12. Piezoelectric cantilever beam displacement.

$V_{OC}$, due to dominant static and conduction power losses. Maximum efficiency of 90.3% is observed for hybrid system at $V_{OC} = 5.5\ V_{PP}$.

## IV. Wearable Energy Harvesting System

In the second experiment, the hybrid harvester structure was built into a wearable prototype to extract power from body movements. The harvester is composed of a conventional

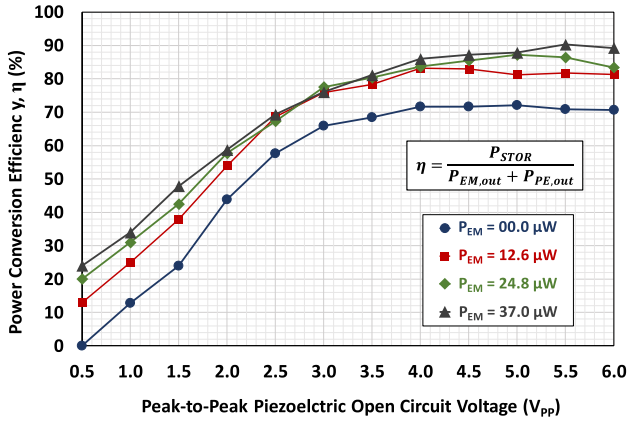


Fig. 13. Experimental power conversion efficiency vs. peak-to-peak piezoelectric open circuit voltage for high frequency excitations.

PE harvester (V22BL) from MIDE Company and a custom-made EM harvester as shown in Fig. 14 (a). PE harvester V22BL has two identical piezoelectric layers with capacitance of $C_{PZT} = 9$ nF on top and bottom of the cantilever beam, and only one of them is utilized in the hybrid system. In the proposed system, base structure of PE harvester is clamped to the lower cap of the EM harvester. A support beam with magnetic tip mass is attached to harvester cantilever beam to translate vertical motion. Hybrid harvester uses low-frequency environmental vibrations to induce higher frequency vibrations at the PE harvester, a phenomenon referred as mechanical frequency up-conversion. This is achieved by imposing initial displacement to piezoelectric cantilever beam. As a result, it begins to vibrate at its damping natural frequency. Damping natural frequency describes vibration frequency of the PE harvester, which starts vibrating by itself after an initial disturbance. Damping natural frequency of PE harvester is observed at 20 Hz, which is 10 times higher than the EM natural frequency of 2 Hz. EM harvester, which can generate power from low frequency vibrations, has a similar structure as the one used in [22]. It contains a fixed magnet at the lower cap in opposite polarity with a free moving magnet inside the cylindrical tube. As the free moving magnet oscillates inside the pick-up coil due to external vibration, an alternating magnetic field induces voltage between two terminals of the pick-up coil according to Faraday's law. On the other hand, when the free magnet gets closer to the lower cap, it pulls up magnetic tip attached to the support beam and consequently deflects cantilever beam. As the free magnet moves downward in the tube, magnetic tip is released and PE harvester starts oscillation at its resonance frequency. This frequency up-conversion enables both harvester to generate energy concurrently.

Fabricated prototype of the hybrid system is presented in Fig. 14 (b–c). Electrical connection pins of harvesters are taken from top of the system in order not to disturb operation of harvesters. The wearable hybrid harvester system was located on the wrist of a jogger as shown in Fig 14(d). Throughout experiments, fundamental vibration frequencies between 2 and 3 Hz were observed for EM harvester placed on the wrist of a jogger as presented in [26]. PE harvester V22BL

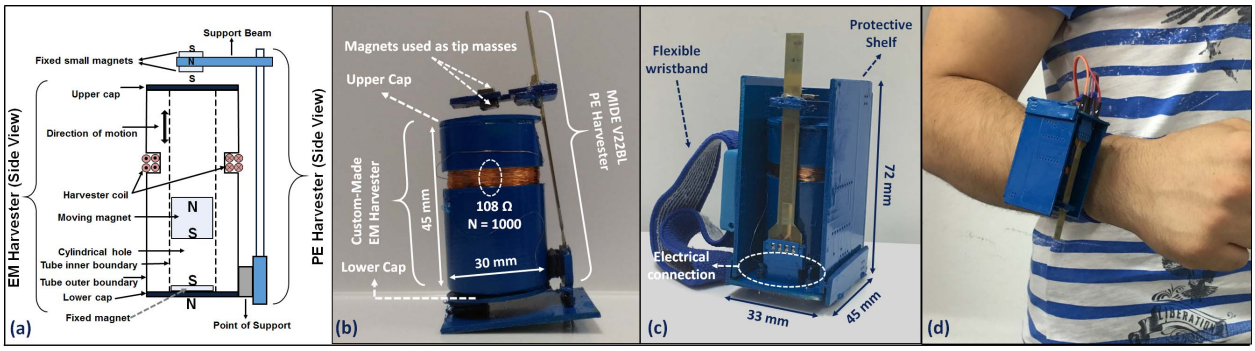


Fig. 14. (a) Schematic of hybrid energy harvester prototype consisting of a PE harvester and custom-made EM harvester. (b) Fabricated prototype of hybrid energy harvester and (c) its protective shelf with flexible wristband adapted for daily usage of the system. (d) Hybrid energy harvester system placed on the wrist of a jogger.

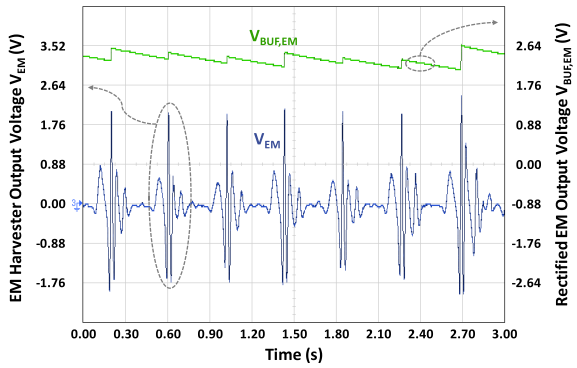


Fig. 15. Measured waveforms of $V_{EM}$ and $V_{BUF,EM}$ with hybrid system operation during jogging.

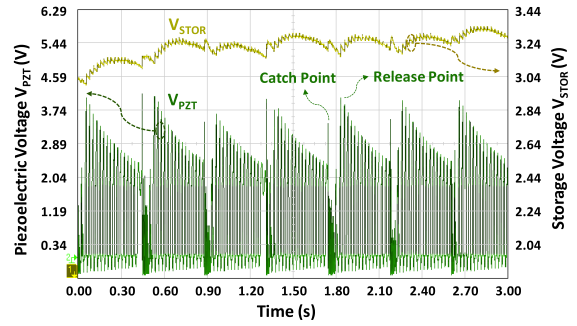


Fig. 16. Measured waveforms of $V_{PZT}$ and $V_{STOR}$ with hybrid system operation during jogging.

was clamped to the base structure, and operates around 20 Hz damping natural frequency with the support beam and the tip mass.

The harvested energy from jogging charges the $C_{BUF,EM}$ as shown in Fig. 15. Fig. 16 presents the measured waveforms of rectified piezoelectric voltage, $V_{PZT}$, and storage voltage, $V_{STOR}$, during jog when 800 kΩ load resistance is connected to storage capacitance. Waveforms of Fig. 15 and Fig. 16 were monitored at different time frames. Fig. 16 demonstrates that PE tip mass is caught by EM magnet before fluctuation of PE beam dies out completely.

As PE displacement attenuates, most of the charge packet transferred to the storage capacitance belongs to the harvested energy by EM. Measured extracted power of the hybrid system and standalone harvesting circuits for various loading conditions are presented in Fig. 17. In standalone operation,

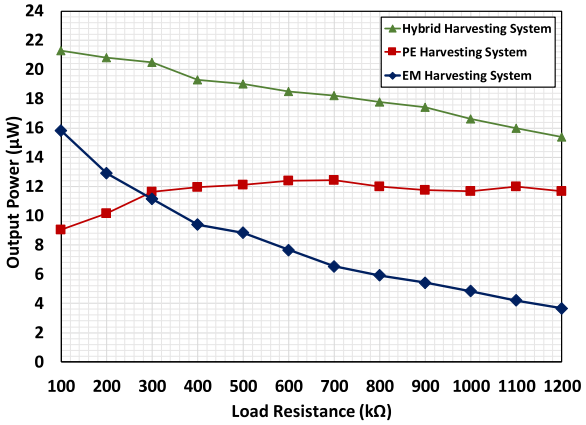


Fig. 17. Experimental extracted power at various loading conditions for excitations during jogging.

the output power of the PE harvester is lower for smaller load resistance, and increases for increasing load resistance, indicating that the losses decrease. Indeed, the conduction losses are dominant for low storage voltage, and degrade as storage voltage increases with higher load resistance. The EM harvesting system delivers more power at lower load resistance, as the load approaches to internal resistance of the EM harvester.

Additional input power in hybrid system increases storage voltage, resulting in reduced on-resistance and thus lower conduction losses. As storage voltage increases with higher load resistance, switching losses start to dominate, and output power degrades in proportion. Hybrid system can deliver almost as much power to the load as the sum of individual PE harvester and EM harvester output power levels. Due to the nature of PE harvester damped vibration, performance of the hybrid circuit degrades for very low amplitudes due to deviation in synchronized points. Moreover, the hybrid system can provide wide storage voltage range of 1 V to 3.4 V while driving resistive load ranging from 100 kΩ to 1200 kΩ.

More power could be generated if the resonance frequency of PE harvester is scaled up through robust design of the mechanical structure. Moreover, dimensions of EM harvester, which occupies most of the hybrid system volume, can be optimized to have a more compact device.

Table I represents the performance of the proposed hybrid harvesting circuit compared with interface circuits in the

TABLE I
COMPARISON OF PROPOSED IC WITH STATE OF THE ART

| Parameters | [10] | [22] | [24] | [16] | [19] | [11] | **This Work** |
|---|---|---|---|---|---|---|---|
| Technology | 0.35 µm | 0.18 µm | 0.18 µm | 0.35 µm | 0.35 µm | 0.35 µm (TEG)<br>0.18 µm (RF) | **0.18 µm HV** |
| Harvesting Sources | PV<br>TEG<br>PE | PE<br>EM<br>TEG | GBFC<br>TEG | PE | PE | TEG<br>RF | **PE**<br>**EM** |
| Excitation Frequencies | PV: DC<br>TEG: DC<br>PE: NA | PE: 282 Hz<br>EM: 2-3 Hz<br>TEG: DC | GBFC: DC<br>TEG: DC | 200 Hz | NA | TEG: DC<br>RF: NA | **PE: 20-500 Hz**<br>**EM: 2-10 Hz** |
| Minimum Input Power | PV: 150 µW<br>TEG: 90 µW<br>PZT: 45 µW | PE: 4.2 µW<br>EM: 1 µW<br>TEG: NA | GBFC: 0.5 µW<br>TEG: 0.5 µW | ≈ 20 µW | 33 µW | TEG: 70 µW<br>RF: NA | **PE: <0.7 µW**<br>**EM: 1 µW** |
| Output Voltage | 1.9 V | 0.8-1.25 V | 1.9 V | 1.8-6.3 V | 1-8 V | 1.75-4.3 V* | **1.1-3.41 V** |
| Max. Conversion Efficiency | NA | 29%<br>@ 68 µW | 85.5%*<br>@ 56.4 µW | NA | 80%*<br>@ 5 mW | 78%<br>NA | **90%**<br>**@ 100 µW** |

PV: Photovoltaic, TEG: Thermoelectric Generator, PE: Piezoelectric, EM: Electromagnetic, GBFC: Glucose Biofuel Cell, RF: Radio Frequency
* It is only for DC-DC circuit.

state-of-the-art literature. The excitation frequencies are limited to harvester components that are provided or fabricated. Operation of the IC has been validated using these limits. The proposed interface circuit for vibration-based harvesters can extract power in a wide vibration frequency range from 2 Hz to 500 Hz. The hybrid operation provides synergistic extraction in a power range of 1 $\mu$W to 100 $\mu$W. Inductor sharing interface circuit in [10] can deliver power to the load from three different input sources, but the interface does not operate below certain input excitation level. Implementations in both [11] and [19] need to overcome the same minimum excitation limitation before they can achieve higher efficiency. The system in [22] cannot generate an output voltage level higher than 1 V due to the low thermoelectric harvester voltage, and high loss in the discrete diodes utilized for combining outputs from different harvesters. Lu *et al.* [16] benefits from MPPT circuits to achieve maximum power transfer through a full-wave rectifier. However, the hybrid IC based on SECE and charge investment technique presented in this work provides higher power capacity, and is efficient for wider range of vibration frequencies. Maximum power conversion efficiency of 90.3% is achieved, which is considerably higher than the state-of-the-art. Besides, the proposed circuit is also adaptable to various harvester types that provides DC output, such as thermoelectric generators, to generate power synergistically with the PE harvester.

## V. CONCLUSION

A hybrid interface circuit for vibration based EM and PE harvesters has been presented. Proposed system can extract energy from multiple sources synergistically to accumulate available energy and improve extracted power. The circuit can handle minimum input power of 1 $\mu$W at wide excitation frequency range from few Hertz to hundreds Hertz. An output voltage range of 1 V to 3.4 V has been attained that is applicable for most of the WSNs. A wearable harvester prototype consisting of custom-made EM harvester, off-the-shelf PE harvester V22BL, and the proposed interface circuit has been built for harvesting energy from body movement. The energy harvesting system can provide up to 20 $\mu$W under different loads during walk action. Due to its relatively small dimension, this system can be placed on mobile animals to sustain WSNs and tracking applications. The proposed hybrid system can efficiently extract available ambient energy, and increase reliability of autonomous micro-devices in WSNs.

## REFERENCES

[1] P. D. Mitcheson, E. M. Yeatman, G. K. Rao, A. S. Holmes, and T. C. Green, "Energy harvesting from human and machine motion for wireless electronic devices," *Proc. IEEE*, vol. 96, no. 9, pp. 1457–1486, Sep. 2008.

[2] R. J. M. Vullers, R. V. Schaijk, H. J. Visser, J. Penders, and C. V. Hoof, "Energy harvesting for autonomous wireless sensor networks," *IEEE Solid-State Circuits Mag.*, vol. 2, no. 2, pp. 29–38, Jun. 2010.

[3] T. Galchev, J. McCullagh, R. L. Peterson, K. Najafi, and A. Mortazawi, "Energy harvesting of radio frequency and vibration energy to enable wireless sensor monitoring of civil infrastructure," *Proc. SPIE*. vol. 7983, Apr. 2011, Art. no. 798314.

[4] M. Fojtik *et al.*, "A millimeter-scale energy-autonomous sensor system with stacked battery and solar cells," *IEEE J. Solid-State Circuits*, vol. 48, no. 3, pp. 801–813, Mar. 2013.

[5] C. Lu, V. Raghunathan, and K. Roy, "Efficient design of micro-scale energy harvesting systems," *IEEE J. Emerg. Sel. Topics Circuits Syst.*, vol. 1, no. 3, pp. 254–266, Sep. 2011.

[6] E. E. Aktakka and K. Najafi, "A micro inertial energy harvesting platform with self-supplied power management circuit for autonomous wireless sensor nodes," *IEEE J. Solid-State Circuits*, vol. 49, no. 9, pp. 2017–2029, Sep. 2014.

[7] S. Du and A. A. Seshia, "A fully integrated split-electrode synchronized-switch-harvesting-on-capacitors (SE-SSHC) rectifier for piezoelectric energy harvesting with between 358% and 821% power-extraction enhancement," in *IEEE Int. Solid-State Circuits Conf. (ISSCC) Dig. Tech. Papers*, Feb. 2018, pp. 152–154.

[8] H. Uluşan, K. Gharehbaghi, O. Zorlu, A. Muhtaroğlu, and H. Külah, "A fully integrated and battery-free interface for low-voltage electromagnetic energy harvesters," *IEEE Trans. Power Electron.*, vol. 30, no. 7, pp. 3712–3719, Jul. 2015.

[9] M. Stoopman, S. Keyrouz, H. J. Visser, K. Philips, and W. A. Serdijn, "Co-Design of a CMOS rectifier and small loop antenna for highly sensitive RF energy harvesters," *IEEE J. Solid-State Circuits*, vol. 49, no. 3, pp. 622–634, Mar. 2014.

[10] S. Bandyopadhyay and A. P. Chandrakasan, "Platform architecture for solar, thermal, and vibration energy combining with MPPT and single inductor," *IEEE J. Solid-State Circuits*, vol. 47, no. 9, pp. 2199–2215, Sep. 2012.

[11] H. Lhermet, C. Condemine, M. Plissonnier, R. Salot, P. Audebert, and M. Rosset, "Efficient power management circuit: From thermal energy harvesting to above-IC microbattery energy storage," *IEEE J. Solid-State Circuits*, vol. 43, no. 1, pp. 246–255, Jan. 2008.

[12] N. J. Guilar, R. Amirtharajah, P. J. Hurst, and S. H. Lewis, "An energy-aware multiple-input power supply with charge recovery for energy harvesting applications," in *IEEE Int. Solid-State Circuits Conf. (ISSCC) Dig. Tech. Papers*, Feb. 2009, pp. 298–299.

[13] H. Uluşan, O. Zorlu, A. Muhtaroğlu, and H. Külah, "Highly integrated 3 v supply electronics for electromagnetic energy harvesters with minimum 0.4 $V_{\mathbf{peak}}$," *IEEE Trans. Ind. Electron.*, vol. 64, no. 7, pp. 5460–5467, Jul. 2017.

[14] C. Peters, J. Handwerker, D. Maurath, and Y. Manoli, "A sub-500 mv highly efficient active rectifier for energy harvesting applications," *IEEE Trans. Circuits Syst. I, Reg. Papers*, vol. 58, no. 7, pp. 1542–1550, Jul. 2011.

[15] L. Wu, X. D. Do, S. G. Lee, and D. S. Ha, "A self-powered and optimal SSHI circuit integrated with an active rectifier for piezoelectric energy harvesting," *IEEE Trans. Circuits Syst. I, Reg. Papers*, vol. 64, no. 3, pp. 537–549, Mar. 2017.

[16] C. Lu, C. Y. Tsui, and W. H. Ki, "Vibration energy scavenging system with maximum power tracking for micropower applications," *IEEE Trans. Very Large Scale Integr. (VLSI) Syst.*, vol. 19, no. 11, pp. 2109–2119, Nov. 2011.

[17] L. Chao, C.-Y. Tsui, and W.-H. Ki, "A batteryless vibration-based energy harvesting system for ultra low power ubiquitous applications," *IEEE Int. Symp. Circuits Syst.*, pp. 1349–1352, May 2007.

[18] D. Kwon and G. A. Rincón-Mora "A single-inductor 0.35 $\mu$m CMOS energy-investing piezoelectric harvester," *IEEE J. Solid-State Circuits*, vol. 49, no. 10, pp. 2277–2291, Oct. 2014.

[19] M. Shim, J. Kim, J. Jeong, S. Park, and C. Kim, "Self-powered 30 $\mu$W to 10 mW piezoelectric energy harvesting system with 9.09 ms/V maximum power point tracking time," *IEEE J. Solid-State Circuits*, vol. 50, no. 10, pp. 2367–2379, Oct. 2015.

[20] J. Sankman and D. Ma, "A 12-$\mu$W to 1.1-mW AIM piezoelectric energy harvester for time-varying vibrations with 450-n$AI_Q$," *IEEE Trans. Power Electron.*, vol. 30, no. 2, pp. 632–643, Feb. 2015.

[21] Y. Sang, X. Huang, H. Liu, and P. Jin, "A vibration-based hybrid energy harvester for wireless sensor systems," *IEEE Trans. Magn.*, vol. 48, no. 11, pp. 4495–4498, Nov. 2012.

[22] U. H. Chamanian, S. Pathirana, W. P. M. R. Pathirana, Ö. Zorlu, O. Muhtaroğlu, and A. Külah, "A triple hybrid micropower generator with simultaneous multi-mode energy harvesting," *Smart Mater. Struct.*, vol. 27, no. 1, Dec. 2018.

[23] R. Ambrosio, R. Torrealba, J. F. Guerrero-C, V. González, A. Limon, and M. Moreno, "Energy harvesting combining three different sources for low power applications," in *Proc. IEEE 12th Int. Conf. Elect. Eng. Comput. Sci. Autom. Control*, Oct. 2015, pp. 12–17.

[24] J. Katic, S. Rodriguez, and A. Rusu, "A high-efficiency energy harvesting interface for implanted Biofuel cell and thermal harvesters," *IEEE Trans. Power Electron.*, vol. 33, no. 5, pp. 4125–4134, May 2018.

[25] S. Chamanian, H. Uluşan, A. Koyuncuoğlu, A. Muhtaroğlu, and H. Külah, "An adaptable interface circuit with multistage energy extraction for low-power piezoelectric energy harvesting MEMS," *IEEE Trans. Power Electron.*, vol. 34, no. 3, pp. 2739–2747, Mar. 2019.

[26] S. Chamanian, H. Uluşan, H. Zorlu, and H. Külah, "Wearable battery-less wireless sensor network with electromagnetic energy harvesting system," *Sens. Actuators A, Phys.*, vol. 249, pp. 77–84, Oct. 2016.


**Salar Chamanian** (M'17) received the B.Sc. and M.Sc. degrees (Hons.) in electrical and electronics engineering from the University of Tabriz, Tabriz, Iran, in 2009 and 2012, respectively, and the Ph.D. degree in electrical engineering from Middle East Technical University (METU), in 2018. He is currently a Research Fellow with the Department of Electrical Engineering, METU. His research interests include CMOS integrated circuit design for low power applications, interface electronics for energy harvester systems, sensors and actuators, power management circuit for wireless sensor network, and MEMS-based energy harvesters.

**Berkay Çiftci** (S'19) received the B.Sc. degree in electrical and electronics engineering from Middle East Technical University (METU), Ankara, Turkey, in 2017, where he is currently pursuing the M.Sc. degree in electronics engineering. He was a Research and Teaching Assistant with METU. He is currently involved in design of interface electronics and power management circuits for MEMS-based energy harvesters. His research interests include integrated circuit design for low-power wearable and implantable applications.

**Hasan Uluşan** (M'12) received the B.Sc. and M.Sc. degrees in electrical and electronics engineering and the Ph.D. degree in electrical engineering from Middle East Technical University, Ankara, Turkey, in 2011, 2013, and 2018, respectively. His research interests include the integrated circuit design especially for low power applications, power management circuits for energy harvesting systems, and mixed-signal circuits and systems for wearable and implantable medical applications.

**Ali Muhtaroğlu** (SM'06) received the B.S. degree from the University of Rochester in 1994, the M.S. degree from Cornell University in 1996, and the Ph.D. degree from Oregon State University in 2007, all in electrical engineering. He was with Intel Corporation R&D, in USA, for 11 years before joining the Electrical-Electronics Engineering Department, Middle East Technical University Northern Cyprus Campus, in 2007, as a Faculty Member, where he is currently the Chair the Center for Sustainability. His experience and research interests include integrated circuit design, energy harvesting, and low power system architectures. He has numerous publications, and a number of patents. He has chaired, co-chaired, and served on the technical program committees for various IEEE conferences.

**Haluk Külah** (M'97) received the B.Sc. and M.Sc. degrees (Hons.) in electrical engineering from Middle East Technical University (METU), Ankara, Turkey, in 1996 and 1998, respectively, and the Ph.D. degree in electrical engineering from the University of Michigan, Ann Arbor, in 2003. During his Ph.D., he worked on micromachined inertial sensors and their interface electronics. His interface electronics designs received several awards in design contests organized/sponsored by prestigious institutions including by Design Automation Conference, IBM, Analog Devices, Compaq, and Texas Instruments. From 2003 to 2004, he was a Research Fellow with the Department of Electrical Engineering and Computer Science, University of Michigan. He joined the Electrical and Electronics Engineering Department, METU, as a Faculty Member in 2004. He has also been the Deputy Director of METU-MEMS Research and Applications Center since 2008. His research interests include MEMS, MEMS-based energy scavenging, microsystems for biomedical applications, and mixed-signal interface electronics design for MEMS sensors. He has more than 130 international publications, 23 national/international patents, and eight international patent applications. He was a recipient of the 2009 Research Encouragement Award by Prof. Mustafa PARLAR Education and Research Foundation, the 2013 Research Encouragement Award by TüBİTAK, the 2013 IBM Faculty Award, and the 2015 Young Scientist Award by Turkish Science Academy. He has received 2015 ERC Consolidator Grant by FLAMENCO project, which on autonomous and fully implantable cochlear implants.